Int. J. Electrochem. Sci., 13 **(2018)** 2022 – 2032, doi: 10.20964/2018.02.69

International Journal of
ELECTROCHEMICAL
SCIENCE
www.electrochemsci.org

Study on Accelerated Stress Test for Fuel Cell Lifetime

Tian Tian, Jianjun Tang, Yanan Chen, Jinting Tan[*]*, Shang Li, Mu Pan*[*]

State Key Laboratory of Advanced Technology for Materials Synthesis and Processing, Wuhan University of Technology, Luoshi Road 122#, Wuhan 430070, PR China
[*]E-mail: 12506@whut.edu.cn panmu@whut.edu.cn

Received: 9 October 2017 / *Accepted:* 11 December 2017 / *Published:* 28 December 2017

A practical accelerated stress test (AST) has been established to analyze the fuel cell durability in this work, which combines the actual operated conditions in fuel cell vehicle. And the durability of two MEAs with different Pt loadings have been studied via this AST. The results show that this AST could effectively decay the MEAs in a short time. After cycling, the thicknesses of the catalyst layers (CLs) reduce and the sizes of the Pt particles grow up compared to the fresh one. The performance decay is mainly attributed to electro-chemical surface area (ECSA) degradation in this work. And in our experiments and experience, ECSA less than 100 cm^2/cm^2 is speculated to be not conducive to stable performance for fuel cell.

Keywords: MEA, durability, accelerated stress test, ECSA, particle size

1. INTRODUCTION

Proton exchange membrane fuel cells (PEMFCs) are recognized as one of the most up-and-coming energy-converting devices, outputting electrical energy through electrochemical reactions without generation of pollutants. [1-2] However, the relatively short lifetime of PEMFCs is still a bottleneck for stationary and automotive applications. [3,4] Apparently, real lifetime experiments will spend much cost and it is inefficiency to satisfy the requirement of the fuel cell technique progress.

For automobile applications, PEMFCs must operate under versatile conditions, such as load changing cycles, high power conditions, idling conditions, and start-up and shutdown cycles. [5] Therefore, it is necessary to establish a practical protocol with various conditions to simulate the real road driving conditions for automotive, in order to better predict the PEMFCs lifetime and analyze the potential degradation mechanism. [6-9] Accelerated stress test (AST) method for PEMFCs lifetime is imperative to be proposed. In theory, an AST for 200 h is equivalent to lasting for 3 years under actual operation condition. [10] The key point of AST for lifetime is that the test protocol must follow actual

running condition and has an ability to accelerate aging. [10] Compared to real lifetime experiments, ASTs occur at more stressful condition to accelerate the failure mode. After a long period of exploration and research, there are a series of AST methods, such as humidity cyclic test [11,12], open circuit voltage (OCV) test [13], load cycle test [14], voltage cyclic test [15], start-stop cyclic test [16], and so on. For example, a AST protocol was reported by Tongji University, which emphasized the OCV-Load cycle lasted for 19.7h, and the performance of PEMFC declined about 13% at 500 mA/cm2 after 200 driving cycles. [17] Tsinghua University has reported a membrane electrode assembly (MEA) durability protocol which contained three types of discharge current density of 0.02 A/cm2, 0.1 A/cm2 and 1.2 A/cm2 and concluded that the major failure factor of the MEA is pinholes degradation of proton exchange membrane due to increased hydrogen gas cross-over. [18] These ASTs have been proved to be a valuable tool for remarkably accelerating degradation of PEMFCs and shortening the lifetime experiments period. [19] However, most accelerate stress tests only consider several conditions, the load on FC stack frequently changes during running especially in vehicular application.

As a core component of PEMFC, MEA is consisted of catalyst coated membrane (CCM), proton exchange membrane and gas diffusion layer (GDL), its durability determines the real-life time of PEMFC or stacks. Therefore, it is essential to establish the reliable method to evaluate the durability of the MEA. [20] In this work, we have established a practical durability measurement system AST to accommodate practical application of PEMFCs. And two MEAs with different Pt loadings and contents have been assembled to explore the performance and durability via AST. The characterizations of MEAs before and after accelerated test were carried out to analyze the material degradation and evaluate this AST protocol.

2. EXPERIMENTAL

2.1. Preparation of MEAs

In this experiment, two standard MEAs with different Pt loadings were produced by Wuhan New Energy Co., Ltd. Each active area of MEAs was 25 cm^2, and the PEM was Nafion211 thin film. When 60% Pt/C commercial catalyst solution was coated on Nafion211, the sample was denoted as C8 with Pt loading of 0.4 mg/cm^2 both in anode and cathode catalyst layer (CL). While 60% Pt/C commercial catalyst solution was used for cathode CL and 20% Pt/C for anode CL, the sample was denoted as C4. Correspondingly, the Pt loading in cathode CL of C4 was 0.3 mg/cm^2, and 0.1 mg/cm^2 Pt loading in anode CL.

2.2 Single cell assembly and measurement equipment

The single cells were self-assembled with current collectors, single snake-type flow channel, Teflon seals. Afterwards, the gas leakages were verified by using N_2 gas (D08-1DM/ZM, Wuhan WUT New Energy Co., Ltd), which were less than 0.2 mL/min both in cathode and anode gas passage.

In this experiment, the fuel cells performance was measured on the G50 fuel cell test platform (Canada Greenlight Company, Canada). Characterization of cyclic voltammetry (CV) was performed using the AUTOLAB electro-chemical workstation (PGSTA30, Netherlands), from 0.05 to 1.25V with a scan rate of 50 mV/s (The single station test delivered H_2/N_2 at 200/200 sccm at 30°C, 100% RH), the linear sweep voltammetry (LSV) curve was conducted from 0 to 0.7 mV at 2 mV/s. Scanning electron microscopy (SEM) images of the MEA were examined by a ULTRA PLUS-43-13 microscope (Carl Zeiss Jena, Germany) to probe the morphological changes of the electrodes and the connection between catalyst layers and membrane. Transmission electron microscope (TEM) images were obtained with a JEM2100F microscope (JEOL, Japan). TEM was used to observe the particle size and distribution of Pt/C particles. Catalyst was removed from the membrane by scraping the catalyst layer and suspending the powder in ethanol solution.

2.3 Durability measurement AST

The schematic plot of AST in this work is shown in Fig.1. This dynamic running cycles are analogous to actual operation of vehicle internal engine. The detail of accelerated test operating condition is shown in Tab.1. It was comprised of 7 working conditions (OCV, idling, rated output, overload, idling-rated cycle, idling-overload cycle and OCV-idling cycle) lasted for 430 min. OCV condition was pointed out at the start and end stages in AST to simulate the start and stop condition in the fuel cell vehicle, idling condition simulates the membrane and catalyst damage in the fuel cell vehicle. Overload was always existed when the FCV run on the road and accelerating degradation. Moreover, since diverse running conditions may exist simultaneously, actual running conditions of fuel cell vehicles are very complex. The idling-rated cycle condition, idling-overload cycle condition and OCV-idling cycle condition are designed in this protocol. High voltage, load cycle and humility cycle will be effective way to accelerate aging.

It was reported that the degradation of the MEA occurred under low-humidification or no humidification conditions of reactant gases. [6] In addition, the fuel cell easily suffers water flooding if it works under a saturated humidification. [7] The frequent humidity cycle will accelerate the degradation of the PEM and catalyst layer. Therefore, the OCV, idling condition and OCV-idling condition were accompanied with 30% humidification, the humidity in other conditions is set at 70%.

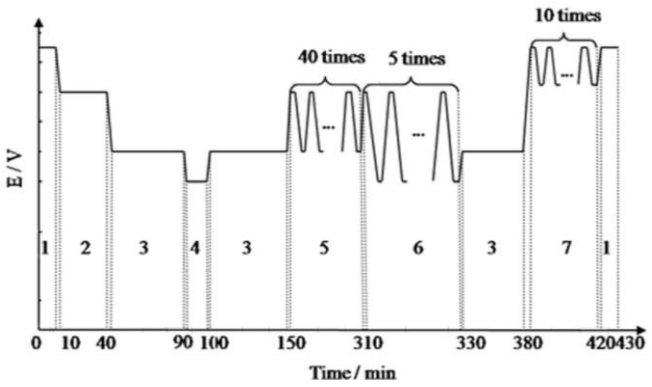

Figure 1. The schematic plot of AST.

Table 1. Test condition of simulated protocol.

Number	Operation Condition	Voltage/V	Humidity/%	Time/min
1	OCV	OCV	30	10
2	Idling	0.8	30	30
3	Rated output	0.6	70	50
4	Overload	0.5	70	10
5	Idling-rated cycle	0.6, 0.8	70	160 (40 times cycle, intervals of 2 min idling)
6	Idle-overload cycle	0.8, 0.5	70	20 (5 times cycle, intervals of 2 min idling)
7	OCV-Idling cycle	OCV, 0.8	70	20 (10 times cycle, intervals of 2 min idling)

Before the vehicle accelerated test, the fuel cell was activated by 3 times cycle test until the performance to a stable state. Anode and cathode were both 100% humidified at a temperature of 65°C, and the stoichiometric ratio of H_2/Air was 1.5/2.5. The electronic load of fuel cell was kept at 600 mA/cm^2 for 6 h until the potential of the fuel cell was no longer increased.

After the activation process, the accelerated test conditions are controlled according to Tab.1. the C8 and C4 were tested for 13 and 23 cycles, respectively, the evolution of voltages related to the cycles presented the transient response to change of dynamic load. But the evolution of voltage will neither lead to a profound understanding of the degradation mechanism, nor provide knowledge of the performance degradation rates. Therefore, polarization curves, cyclic voltammetry curves and linear sweep curves were recorded further.

3. RESULTS AND DISCUSSION

The effect of test cycles on the performance of single cells and the performance degradation of the two sample, respectively, at 200, 600 and 1000 mA/cm^2 current densities are presented in Fig.2. According to Fig. 2(a), the initial performance of the sample C4 was 0.596 V and C8 had an initial performance of 0.616 V at 1000 mA/cm^2. The performance of the cell decreased with increasing testing cycles, voltage of 0.532V was obtained at 1000 mA/cm2 after 23 cycles for C8, and 0.38V after 13 cycles for C4. Durability is defined by the US Department of Energy (DOE) as projected hours to 10% voltage degradation. [21] The voltage degradation of C8 was larger than 10% at high current density testing after 23 cycles, while the C4 only need test for 13 cycles.

The fuel cell performance decreased gradually with increasing cycle testing, the degraded rates of C8 at 200, 600 and 1000 mA/cm^2 current density were 1.00, 1.85 and 2.24 mV/cycle, respectively. The degraded rates increased with increasing current densities. This was attributed to the decrease of the ECSA of Pt catalyst after operating under simulated cycles. With the reduction of the ECSA, the Pt catalyst cannot provide enough active sites for electrochemical reaction at a high current density and consequently causes a decrease in cell performance. In the range of low current densities, the needed active sites of the Pt catalyst are lower than those at high current densities, and, hence, there is no significant degradation in performance. [22] For the sample C4, there were the degraded rate of 3.79, 5.64, 7.46 mV/cycle at 200, 600 and 1000 mA/cm2 current density during 9 testing cycles. However, after testing for 9 times, the potentials decreased sharply, with the degraded rates up to 11.25, 28.1, 38.5 mV/cycle.

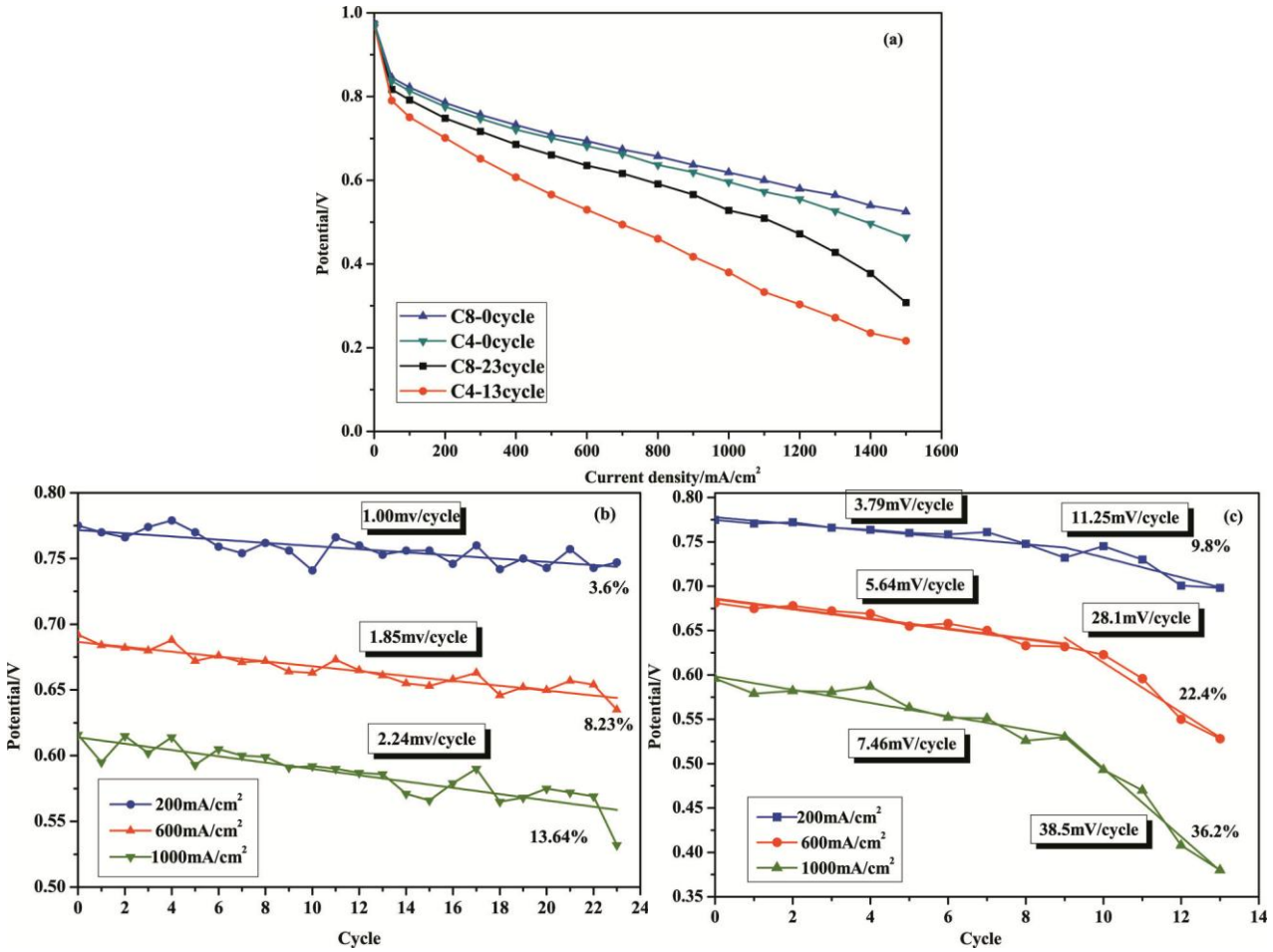

Figure 2. (a) Current-voltage characteristics of initial and test after 13 cycles and the performance degradation of (b) C8 after 23 cycles testing, (c) C4 after 13 cycles under current density of 200 mA/cm^2, 600 mA/cm^2 and 1000 mA/cm^2.

The resistance of PEMFCs during the testing was always below 2.5 mΩ as shown in Fig.3, which assures good contact between each component in MEA.

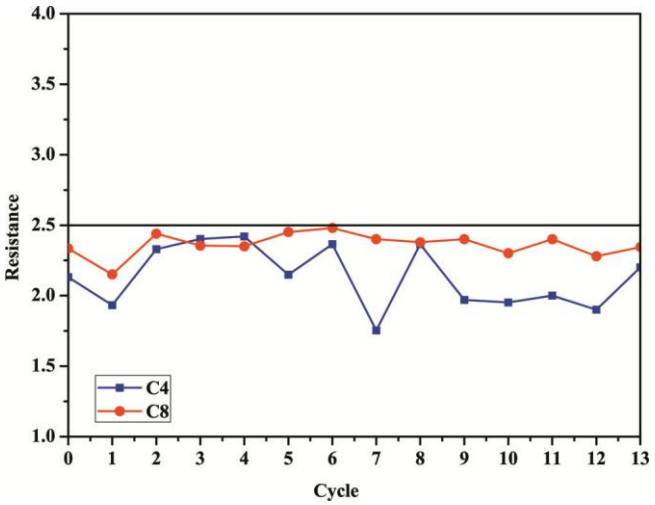

Figure 3. The resistance of the single fuel cell operated after various cycles.

Hydrogen permeation currents are almost unchanged in the range of 0.4-0.7 V (Fig.4). This has proved that the degradation rate of catalyst is much faster than the PEM, and the PEM damage in MEA is not a major degradation factor for performance in this work.

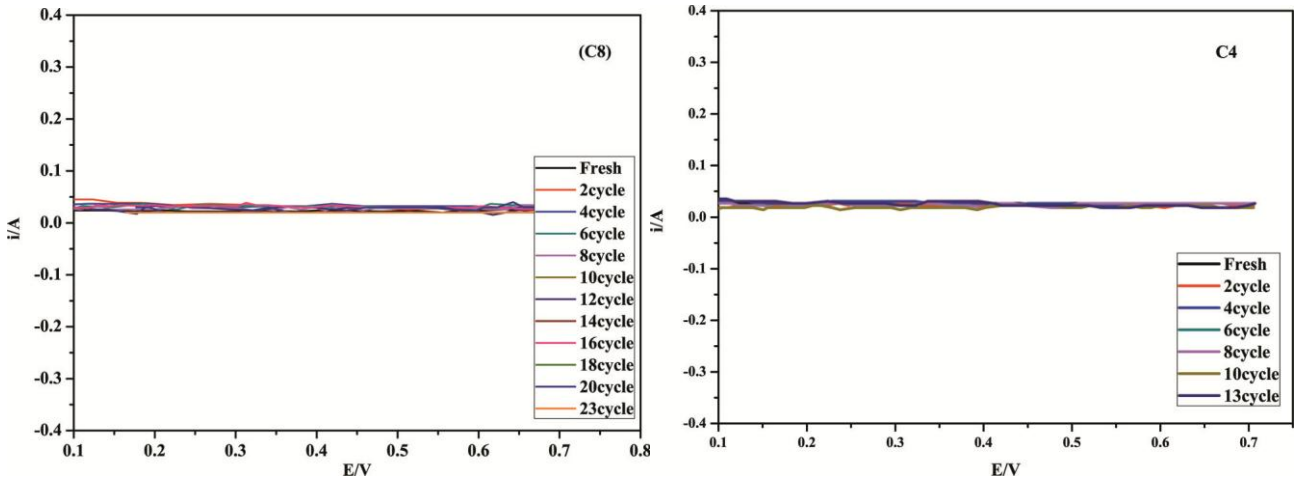

Figure 4. The linear sweep voltammetry curve of fuel cell after each durability test cycle.

The cross-section morphology for fresh and the degraded MEAs is displayed in Fig.5. The characterization of membrane and CL before and after the test protocols have been summarized in the table 2. It is found that the thicknesses of membranes have no change, which are both 24 μm for fresh and the degraded MEAs, a similar degradation phenomenon was reported by Lin[23]. The thicknesses variation for the cathode and anode CL of C8 were 4 and 3μm respectively, which are only both 1.5 μm for C4. That is mainly because that the C8 was operated under a longer time than C4, and the carbon corrosion of C8 was more serious than C4. Furthermore, the cathode catalyst layer had suffered from more corrosion than anode, this is mainly because that the cathode support was in a higher potential circumstance than anode support, which may result in a loss in the number of active sites and hence a decrease of ECSA, and this will in turn lead to performance deterioration in PEM fuel cells.

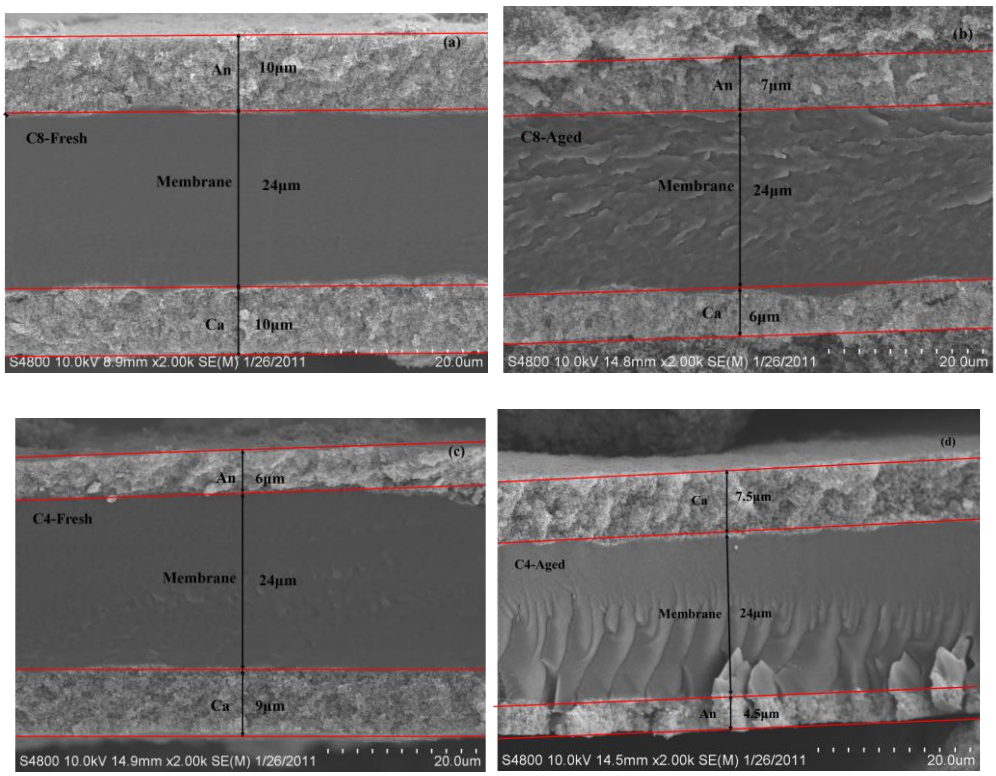

Figure 5. Across-section morphology of two MEAs, (a) fresh C8, (b) aged C8, (c) fresh C4, (d) aged C4.

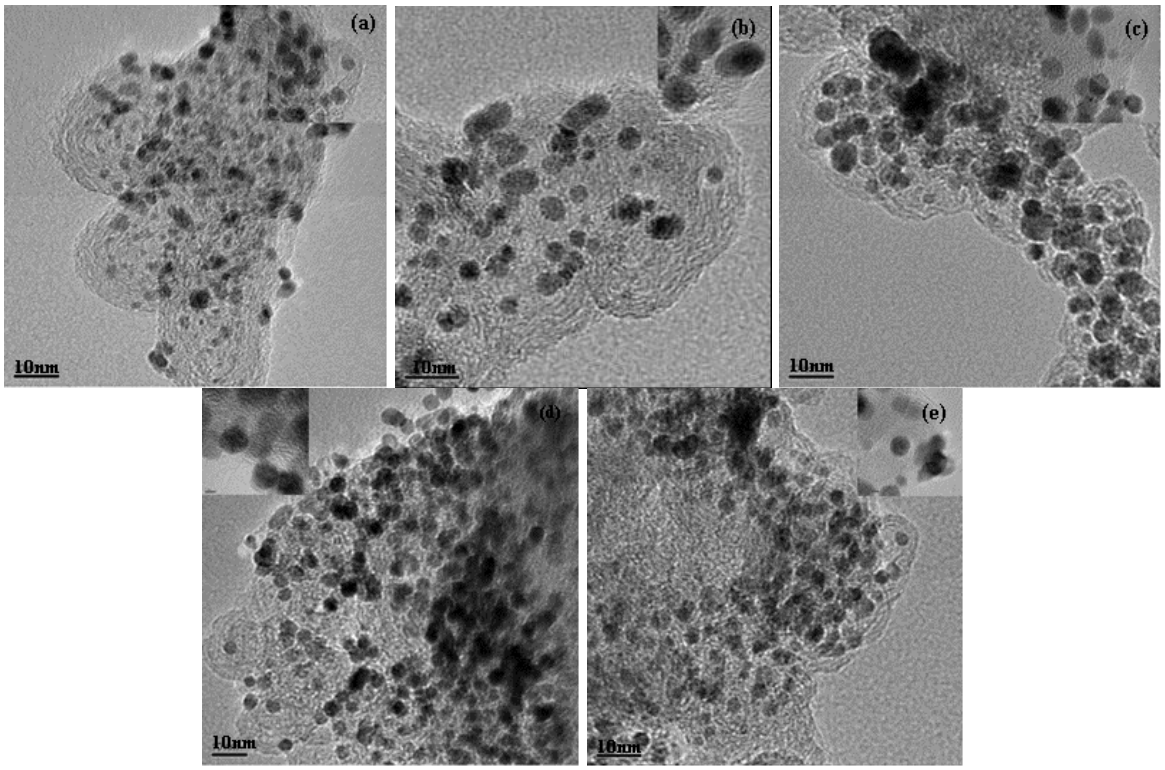

Figure 6. TEM images for CL (a) fresh, (b) cathode and (c) anode for aged C8, (d) cathode and (e) anode for aged C4.

Fig.6 is the TEM images of the fresh and degraded catalyst. For the fresh MEA, Pt particles with size of 3 nm are uniformly dispersed on the carbon support. After cycles, the particles sizes of catalysts in either anode or cathode electrodes obviously grow up. The average Pt particle size for anode in the C8 CL is about 4.5 nm, while the C4 is about 3.5 nm. This indicates that high Pt loading and content will accelerate particle agglomerate. Another interesting founding is that particle growth for cathode catalyst is much faster than anode, which are 5.5 and 5.0 nm for C8 and C4 respectively. Furthermore, the change geometric shape is observed, and it occurs after cycling for Pt particles. Many irregular Pt particles are seen in the CL, while more spherical Pt particles is present in fresh CL. Dissolution and recrystallization of Pt could explain for this observation. In other words, Pt in the catalyst layer may be oxidized to ions. These mobile Pt ions could be induced to form the irregular particles, which would be a thermodynamically favorable process. [24]

Table 3. Characterization of the MEA and CL before and after the test protocol through SEM, TEM

Test	SEM Thickness (μm)				TEM Mean Pt particle size (nm)	
	Cathode	Anode	Membrane	CCM	Cathode	Anode
C8-Fresh	10	10	24	44	3.0	3.0
C8-Aged	6	7	24	37	5.5	4.5
C4-Fresh	9	6	24	39	3.0	3.0
C4-Fresh	7.5	4.5	24	37.5	5.0	3.5

The electro-chemical surface area (ECSA) is one of the most valuable parameters for characterizing the catalytic activity which affects the performance of PEM fuel cell. [16,25] As shown in Fig.7, there was a similar degraded rate of ECSA in the cathode CLs of C8 and C4, while in the anode CL of C8, the degradation of ECSA has occurred quite rapidly during the first 9 cycles. That is because that the 60% Pt/C was used in CL, high Pt loading and content will accelerate particle coalescence during aging in addition to accelerating Pt particle growth and loss of ECSA.

The performance degraded of C4 was more serious than the C8, especially after testing for 9 cycles. According to our experience, there is a threshold value (100 cm^2/cm^2) of ECSA in the CL (Pt/C, carbon black nanoparticles Vulcan XC72). When the ECSA of CL less than 100 cm^2/cm^2, the performance of fuel cell decreases sharply. Therefore, the cathode ECSA of C4 was only about 100 cm^2/cm^2 after aging 9 cycles during this test protocol, a rapid degradation rate of performance can be observed.

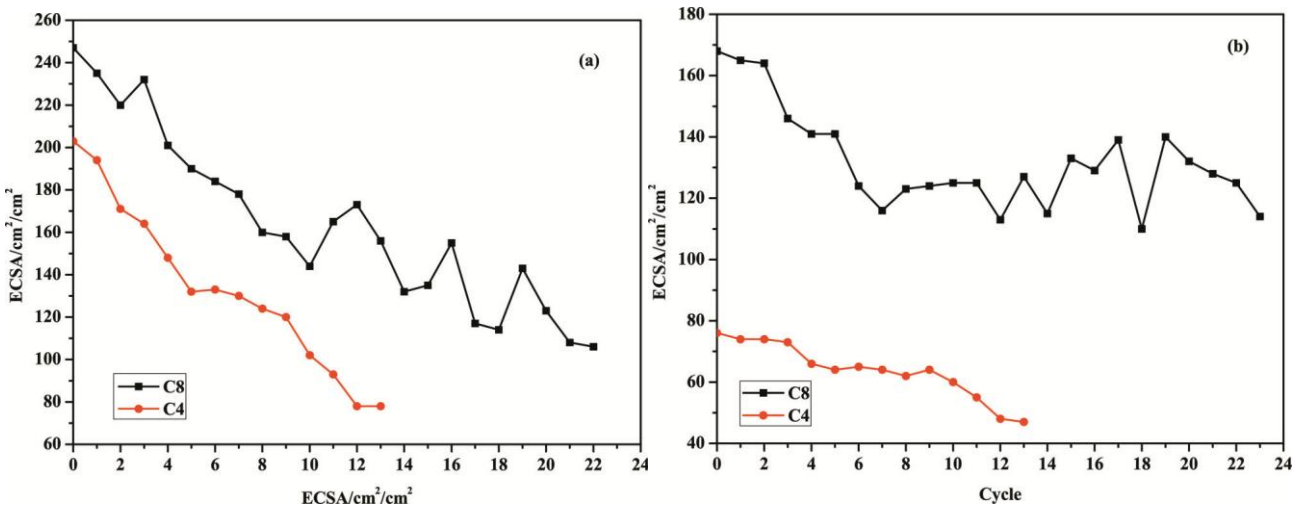

Figure 7. ECSA versus different cycle in the (a) cathode and (b) anode of MEA.

The evolution of rough factor versus Pt loading in theory has been shown in Fig.8. According to this figure and considering the utilization and durability of Pt, the Pt loading of 0.2 mg/cm^2 in the cathode with a ECSA is larger than 100 cm^2/cm^2 and is enough for a fuel cell, which is in accordance with the report that assembled fuel cell with Pt-loading of 0.05 mg/cm^2 in anode proved no significant voltage losses, and that with Pt loading of 0.2 mg/cm^2 in cathode exhibited an excellent performance (10-20 mV voltage losses). [26-28]

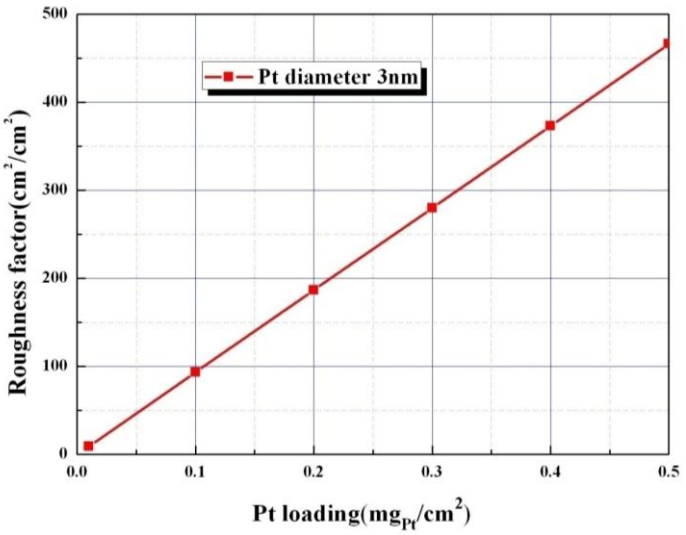

Figure 8. Evolution of rough factor versus Pt loading

Based on the above statement for the two MEAs, a MEA with a high Pt loading could be destroyed after 23cycles about 165h, and a relatively low Pt loading only need 13cycles (93h). That indicates that compared to other researches,[17,18,29,30] our protocol is an efficient method to simulate the actual operating environment of the fuel cell vehicle, and can accelerate aging in a short

time. In this AST protocol, voltage control mode was adopted that could accelerate achieve catalyst decay and carbon corrosion, compared with current control and power control. This method strengthens cycles to accelerate aging of MEA which is suitable to study the durability of MEA in order to improve it.

4. CONCLUSION

In this work, a practical AST has been put forward to evaluate the durability of MEA in a short time. Two MEAs with different Pt loadings and contents have been studied using this AST protocol, and both MEAs have been decayed. The one with a high Pt loading has been aged after 165h with a 0.09 V potential decrease at 1000 mA/cm^2, while the other one only needs 93 h (0.21 V potential decrease). The SEM result revealed that the thickness change of CL with the high Pt loading and content was more serious than the other one after AST cycle test. And the Pt particles in the high Pt loading CL were more likely to agglomerate after AST cycles. All the results indicate that AST protocol is an efficient method to simulate the actual operating environment of the fuel cell vehicle which could accelerate aging in a short time. After testing for 9 cycles, potential of the fuel cell decreases rapidly in accordance with our experience when the ECSA less than 100 cm^2/cm^2 will lead to an unstable performance in fuel cell.

ACKNOWLEDGEMENT
This work was financially supported by the National Key Research and Development Program of China (Program No. 2016YFB0101200 (2016YFB0101205)) and Hubei Province Technology Innovation Project (Program No. 2016AAA047).

References

1. M. Lopezharo, L. Guétaz, T. Printemps, A. Morin, S. Escribano, P.H. Jouneau, P. Bayle-Guillemaud, F. Chandezon and G. Gebel, *Nat. Commun.*, 5 (2014) 5229.
2. M. K. Debe, *Nature*, 486 (2012) 43.
3. K. Hartl, M. Hanzlik and M. Arenz, *Energ. Environ. Sci.*, 4 (2010) 234.
4. Y. Yu, H. Li and H.J. Wang, *J. Power Sources*, 205 (2012) 10.
5. Y. Jeon, H. Na, H. Hwang, J. Park, H. Hwang and Y. Shul, *Int. J. Hydrogen Energy*, 40 (2015) 3057.
6. S. Wasterlain, D. Candusso and F. Harel, *J. Power Sources*, 196 (2011) 5325.
7. X.Z. Yuan, S. Zhang and J.C. Sun, *J. Power Sources*, 22 (2011) 9097.
8. W. Schmittinger, A. Vahidi, *J. Power Sources*, 180 (2008) 1.
9. Y. Jeon, H. Na, H. Hwang, J. Park, H. Hwang and Y.G. Shul, *Int. J. Hydrogen Energy*, 40 (2015) 3057.
10. M. Hicks, P. Dan, P. Turner and T. Watschke, *ECS Trans*, 1 (2006) 229.
11. H. Tang, P. Shen, S.P. Jiang, F. Wang and M. Pan, *J. Power Sources*, 170 (2007) 85.
12. X. Huang, R. Solasi, Y. Zou. M. Feshler, K. Reifsnider, D. Condit, S. Burlatsky and T. Madden, J. *Polym. Sci., Part B: Polym. Phys*, 44 (2006) 2346.
13. A. Ohma, S. Yamamoto and K. Shinohara, *J. Power Sources*, 182 (2008) 39.
14. F. Rong, C. Huang, Z.S. Liu, D. Song and Q. Wang, *J. Power Sources*, 175 (2008) 699.
15. K. Yasuda, A. Taniguchi, T Akita, T Ioroi and Z. Siroma, *Phys Chem Chem Phys*, 8 (2006) 746.

16. J.C. Meier, C. Galeano, I. Katsounaros, A.A. Topalov, A. Kostka, F. Schüth and K.J. J. Mayrhofer *ACS Catal*, 2 (2012) 832.
17. B. Lia, R. Lin, D. Yang and J. Ma, *Int. J. Hydrogen Energy*, 35 (2010) 2814.
18. M. Liu, C. Wang, F. Xie and Z. Mao, *Int. J. Hydrogen Energy*, 38 (2013) 11011.
19. Y. Jeon, S.M. Juon, H. Hwang, J. Park and Y.G Shul, *Electrochim Acta*, 148 (2014) 15.
20. X.Z. Yuan, H. Li, S. Zhang, J. Martin and H. Wang, *J. Power Sources*, 196 (2011) 9107.
21. D.H. Zhong, H. Sano, Y. Uchiyama and K. Kobayashi, *Carbon*, 38 (2000) 1199.
22. Y.C. Park, K. Kakinuma and M. Uchida, *Electrochim Acta*,, 123 (2014) 84.
23. R. Lin, B. Li, Y.P. Hou and J.M. Ma, *Int. J. Hydrogen Energy*, 34 (2009) 2369.
24. J. Xie, D.L. Wood, K.L. More, P. Atanassov and R.L. Borup, *J Electrochem Soc*, 152 (2005) A1011.
25. Y.W. Lee, S.N. Cha, K.W. Park J.I. Sohn and JM Kim, *J Nanomater*, 16 (2015) 1.
26. H.A. Gasteiger, J.E. Panels and S.G. Yan, *J. Power Sources*, 127 (2004) 162.
27. S. Sun, H. Zhang and M. Pan, *Fuel cells*, 15 (2015) 456.
28. A. Kongkanand, N.P. Subramanian, Y. Yu, Z. Liu, H. Igarashi and D.A. Muller, *ACS Catal*, 6 (2016) 1578.
29. R. Petrone, D. Hissel, M.C. Péra, D. Chamagne and R.Gouriveauac, *Int. J. Hydrogen Energy*, 40 (2015) 12489.
30. R. Sharabi, Y.H. Wijsboom, N. Borchtchoukova, G. Finkelshtain and L. Elbaz, *J. Power Sources*, 335 (2016) 56.